EPJ Web of Conferences **318**, 03005 (2025) https://doi.org/10.1051/epjconf/202531803005
AAPM-III 2025

An experimental method for detecting objects in an aqueous environment

Yuri Kuzmin[1], and *Stanislav* Proshkin[2*]

[1]Department of General and Applied Physics, Empress Catherine II Saint Petersburg Mining University, St.-Petersburg, Russia
[2]Department of Physics, Saint-Petersburg State University of Aerospace Instrumentation, St.-Petersburg, Russia

Abstract. This research introduces a novel experimental approach for identifying conductive and non-conductive objects submerged in shallow water using grounded cables. The methodology is underpinned by a comprehensive mathematical analysis of electromagnetic field diffraction caused by elongated conductive and non-conductive spheroids in an aqueous environment, specifically when interacting with a grounded cable. The experimental configuration employs a parallel arrangement of a generator and two receiving electrode antennas. A key feature of this technique is its ability to distinguish an object's unique flow characteristic from ambient noise. This is achieved through the application of digital hardware and software filtering to a modulated sinusoidal signal. To facilitate this process, the researchers developed a specialized algorithm designed to filter out pulse and fluctuation interference. This innovative approach represents a significant advancement in underwater object detection, offering potential applications in various fields such as marine archaeology, environmental monitoring, and underwater infrastructure inspection.

1 Introduction

The foundation for detecting both conductive and non-conductive objects in seawater relies on solving the electromagnetic field diffraction problem of a grounded cable interacting with an elongated spheroid, whether conductive or non-conductive. An elongated non-conductive spheroid serves as an effective model for a diver in a wetsuit [1]. The primary electromagnetic field in seawater is generated by an electrode antenna, specifically a grounded cable. The electric field is primarily determined by free charges on metal electrodes, while the field created by the connecting cable is considered negligible. When this grounded cable's field interacts with a dielectric spheroid, it induces a secondary field. This secondary field can be conceptualized as the combined effect of two equivalent dipoles: one aligned with the spheroid's major semi-axis and another with its minor semi-axis.

In shallow water environments, seawater forms a conductive layer sandwiched between the seabed and the atmosphere. The challenge of determining the secondary field produced by a horizontal dielectric spheroid within this conductive layer has been rigorously addressed

---

* Corresponding author: stach@mail.ru

and solved mathematically [1]. This theoretical framework provides a robust basis for understanding and predicting the behavior of electromagnetic fields in shallow seawater, which is crucial for developing effective detection methods for various underwater objects.

In the experimental implementation of the proposed method for detecting conductive and non-conductive objects in the aquatic environment, it is necessary to solve the problem of isolating relatively slowly changing regular signals (spectrum up to 10 Hz) when exposed to noise and fluctuations of various kinds.

The purpose of this article is a theoretical and hardware solution to the problem of detecting a regular signal received from an underwater swimmer in shallow water. This is achieved by placing the generator and two receiving electrode antennas in parallel and highlighting the passing characteristics of the object against the background of noise by digital hardware and software filtering of the modulated sinusoidal signal.

2 Methods and apparatus

2.1 Mathematical model

If the conductivity of the detected body differs from that of seawater, then when this body enters the field of spreading currents of the transmitting electrode antenna, the primary field of the antenna will be distorted. Moreover, the nature of this distortion depends on the type of conductivity of the detected object. The authors of this article previously developed a mathematical model for determining the distortion of the secondary field by a detectable object in the form of a conductive and non-conductive spheroid in an aqueous medium [1].

Let us examine the secondary electromagnetic field produced by a non-conducting spheroid in a setup where a generator and two receiving electrode antennas of identical length $2l$ are arranged in parallel (as shown in Figure 1).

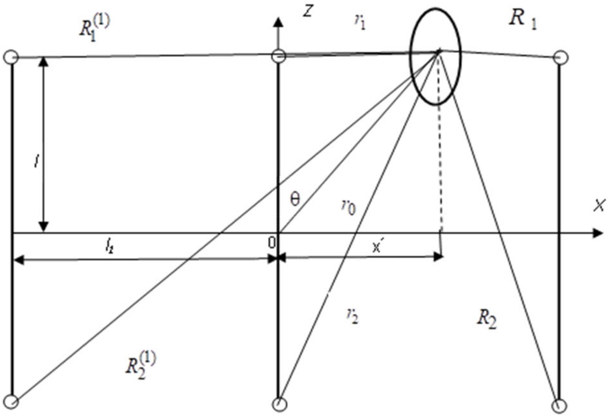

Fig. 1. The layout of the electrode antennas relative to the detected object.

In this configuration, the generator and receiving electrode antennas are aligned along the z-axis. The separation between the generator and receiving electrode antennas is denoted as l_1 .The object under consideration is an elongated spheroid characterized by semi-axes a and c. Based on the geometric layout shown in Figure 1, we can define the following parameters:

- h represents the vertical distance from the reservoir bottom to the spheroid's center;
- r_0 indicates the horizontal distance from the system's center to the spheroid's center;
- the relationship between these parameters is expressed as $\cos\theta = \frac{z}{r_0}$.

This setup allows for the analysis of the electromagnetic field interactions between the antennas and the submerged non-conducting spheroid, which is crucial for detecting and characterizing objects in shallow water environments.

The most likely movement of the object will be parallel to the antennas. From geometry we have $r_{1,2} = \sqrt{r_0^2 + l^2 \mp 2r_0 l\cos\theta}$- the distances from the center of the spheroid to the first and second electrodes of the generator antenna;$R_{1,2} = \sqrt{(z \mp l)^2 + h_2 + (l_1 - x')^2}$- the distances to the corresponding electrodes of the left receiving antenna; $R_{1,2}^{(1)} = \sqrt{(z + l)^2 + h^2 + (l_1 + x')^2}$- the distances to the corresponding electrodes of the right receiving antenna.

The output signal of the receiver adder will be [1]

$$U_\Sigma = -\frac{U_0 bl}{3\pi^2} V_{\text{c}\phi}[(\alpha\alpha_2^- - \beta\beta_2^-) + (\alpha\alpha_2^{-(1)} - \beta\beta_2^{-(1)})]/N_z', \tag{1}$$

where $V_{\text{c}\phi} = (4/3)\pi a c^2$-the volume of the spheroid; *a*- the major semimajor axis; *c*- the minor semimajor axis; $N_z' = \frac{(1-\eta_0^2}{\eta_0^3}(\text{Arth}\eta_0 - \eta_0)$ - the depolarization coefficient along the axis associated with the symmetry of the spheroid; $\eta_0 = \sqrt{1 - \frac{c^2}{a^2}}$- the eccentricity of the spheroid;

$$\alpha = \frac{e^{-x_0}}{r_0^3}[(1 + x_0)\cos x_0 + x_0 \sin x_0];\beta = -\frac{e^{-x_0}}{r_0^3}[(1 + x_0)\, sin\, x_0 - x_0\, cos\, x_0];$$

$$\alpha_2^- = \frac{e^{-x_1}}{R_1^3}[(1 + x_1)\, cos\, x_1 + x_1\, sin\, x_1]\, cos\, \theta_1 - \frac{e^{-x_2}}{R_2^3}[(1 + x_2)\, cos\, x_2 + x_2\, sin\, x_2]\, cos\, \theta_2;$$

$$\beta_2^- = \frac{e^{-x_1}}{R_1^3}[(1 + x_1)\, sin\, x_1 - x_1\, cos\, x_1]\, cos\, \theta_1 - \frac{e^{-x_2}}{R_2^3}[(1 + x_2)\, sin\, x_2 - x_2\, cos\, x_2]\, cos\, \theta_2;$$

where $x_0 = k_0 r_0$, $x_1 = k_0 R_1$, $x_2 = k_0 R_2$ are dimensionless distances expressed in wavelengths in water; $k_0 = \sqrt{(\omega\mu_0\sigma)/2}$- the modulus of the propagation coefficient in water; $cos\, \theta_{1(2)} = -\frac{(z \mp l)}{R_{1(2)}}$- the cosines of the angles between the axis z' and the radii by vectors $\vec{R}_{1(2)}$ drawn from the center of the spheroid to the first and second electrodes of the left receiving antenna.

The functions α_2^{-1} and β_2^{-1} are defined from the functions α_2^- and β_2^- by replacing them $R_{1,2}$ with $R_{1,2}^{(1)}$, then $cos\, \theta_{1(2)}^{(1)} = -\frac{(z \mp l)}{R_{1,2}^{(1)}}$.

2.2 Experimental setup and research results

The security system of the water area is built from separate modules. The created experimental installation of the security system module (Figure 2) contains the following elements: a quadrature generator 1, which creates both a sinusoidal and cosine signal at the output (with a phase difference of 90°); an amplifier 3, connected via an adjustable phase corrector 2. The phase corrector reduces distortion of the waveform as it passes through the circuit, due to the nonlinearity of the phase-frequency response of the circuit. In our case, such distortions are introduced by the amplifier and its output and input connection circuits. The output of the amplifier is connected to the primary electromagnetic field emitter 4, the working part of which is two copper discs spaced along the boundary, thus a linear electrode antenna is obtained.

The receiving channel of the installation contains two similar antennas 5 and 5', signal processing units including differential amplifiers 6, 6' and a summing signal amplifier from two antennas 7. Next, a quadrature synchronous detector 8 allocates quadrature signal components Q and I, which enter a dual integrating filter 9. A low-pass filter with a cutoff frequency of $f_p = 4$kHz is used as an integrator 9. The resulting signal is digitized by a synchronous analog-to-digital converter 10, and the received quadrature signals I and Q are digitally processed by a microcontroller 11. The final information is transmitted to a personal computer using a special interface.

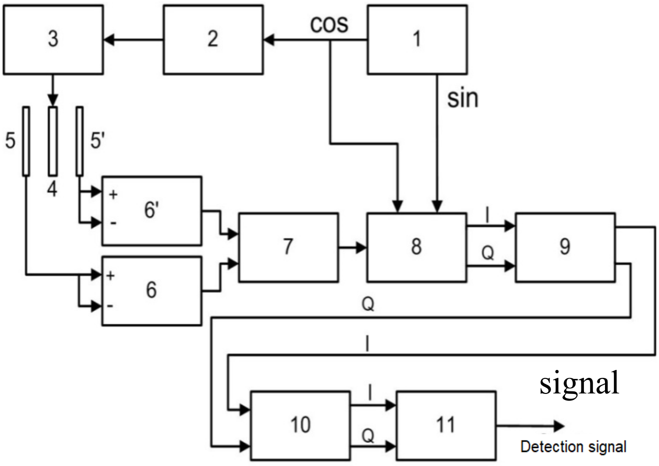

Fig. 2. Block diagram of the experimental installation.

In a personal computer, real-time signal processing takes place using a special program, which performs the following operations: controls the allocation of a useful signal; filtering; detection; making a decision on the detection of an object; classifying an object on the basis of a metal-dielectric and calculating its speed.

The program also controls the main parameters of the receiving device through the interface: gain; data transfer rate; sampling rate, etc.

Since our installation used a transmission line with a cable of about 400 meters, an upgraded RS-232 port turned out to be the most suitable for receiving and processing data in a computer. This data exchange protocol has the following ratios: logical "0" is + 12 V, logical "1" is 12 V. This circumstance made it possible to increase the noise immunity of information in data transmission lines. The serial interface was implemented by a PIC16F873-877 series microcontroller. These microcontrollers use a synchronous asynchronous USART transceiver [2-4].

Figure 3 shows an example of calculating the real parts of the flow characteristics $U_\Sigma(z)$ according to formula (1) for an elongated dielectric spheroid with a volume of 100 liters at $a = 0{,}9$ m; $c = 0{,}3$ m; $h = 3{,}5$ m, $\sigma = 1\,(\mathrm{Om \cdot m})^{-1}$; $f = 4 \cdot 10^3$ Hz; $b = 0{,}125$ m; $U_0 = 20$ V; $l = 5$ m; $l_1 = 4{,}5$ m and four options for passing the object through the protected boundary: $x' = 4{,}5$; 3,0; 1,5; and 0 m corresponding to curves 1, 2, 3, 4 Figure 3. The experimentally obtained curve 1 corresponds to the flow characteristics of an object moving directly above the receiving antenna at $x' = 4{,}5$ m, and curve 4 corresponds to the generator antenna. It is clearly seen from the curves shown in Figure 3 that the shape of the passing characteristics changes very little along the protected boundary in the case of varying the distance between the object and the receiving antennas. In addition, the voltage values of the measured signals in the maxima are close and make it possible to clearly record the passage of the detected object through the protected boundary.

Separately, we note that the flow characteristics in the case of a conductive elongated spheroid will differ from those of a non-conductive spheroid (Figure 3) by a sign of a different polarity and a larger signal magnitude [1]. This circumstance greatly simplifies the preprocessing of signals and their isolation from the background noise.

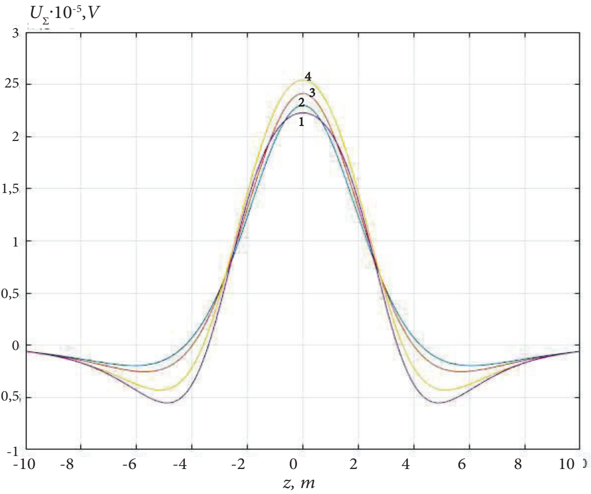

Fig. 3. Flow characteristics of a non-conducting elongated spheroid.

3 Results and discussion

Mathematically, the problem of detecting a regular signal from an underwater swimmer in shallow water conditions was solved in [1]. During the experiment, this occurs due to the isolation of relatively slowly changing regular signals (spectrum up to 10 Hz) under the influence of significant noise and fluctuations of various kinds. Therefore, data preprocessing is one of the urgent tasks that arise when processing signals of various physical nature.

First of all, this task is related to the allocation of a useful signal against the background of interference. It is necessary to separate the useful signal $y[n] = f(x[n], \gamma[n])$ from the interference distorting it based on the signal observed at discrete time points $n = 1,...,N$. It is clear that such a task has a solution only if the type of function $x[n]$ is known in advance, or reasonable assumptions are made about its specific form.

Since in our case the carrier frequency of the signal (4 kHz) is precisely known, this greatly simplifies the processing task. Let's say the analog part of the signal processing is carried out, i.e. frequencies above 4 kHz are filtered to exclude signal oversampling, the signal is digitized (a one-dimensional data array is obtained). It is necessary to filter the carrier frequency from noise and fluctuations and isolate the envelope of the received signal.

First, the signal is preprocessed, in which it is cleared of pulse interference and abnormal counts ("misses"). For this purpose, a specialized algorithm for eliminating "misses" was used, proposed in [5,6] and implemented in the CodeGearRADStudio software environment, in the Paskal language. At the same time, an important factor is that this algorithm removes pulse interference and does not change the statistical properties of the useful signal [7, 8].

Thus, during the preprocessing of the signal, its filtering occurs, which reduces to the detection of a pulse emission and the replacement of abnormal samples with approximated ones. There are many ways to approximate the signal. Since the signal is processed at discrete points in time and the values of the signal at intermediate moments are not defined, we can consider the array of samples as a lattice function. The signal can be approximated by one, two or three last counts.

Approximation by one sample means that the predicted value should be assumed to be equal to the previous one. In the case of two samples, it is assumed that the signal changes linearly. Of particular interest is the approximation based on the three previous counts. In this case, it is assumed that the function changes according to the law of the polynomial of the second degree:

$$x(t) = at^2 + bt + c. \tag{2}$$

In the case of such an approximation, it is necessary to take into account not only the possibility of an increase or decrease in the function, but also the rate of its change, i.e. the magnitude and sign of the first and second derivatives.

The first derivative for lattice functions is defined as follows:

$$\Delta f_n = f_n - f_{n-1}. \tag{3}$$

For the second derivative of the lattice function, we can write:

$$\Delta 2 f_n = \Delta f_n - \Delta f_{n-1} = f_n - 2 f_{n-1} + f_{n-2}. \tag{4}$$

To approximate the next reference, we use the expression:

$$f_{n+1} = f_n + \Delta f_n + \Delta 2 f_n = f_n + (f_n - f_{n-1}) + ((f_n - f_{n-1}) - (f_{n-1} - f_{n-2})). \tag{5}$$

When,

$$f_{n+1} = 3 f_n - 3 f_{n-1} + f_{n-2}$$

Thus, as a result of the approximation, the next count of the useful signal will be equal to:

$$x_{n+1} = 3x_n - 3x_{n-1} + x_{n-2}. \tag{6}$$

The proposed algorithm makes it possible to eliminate impulse and abnormal interference, as a result of which the received signal (6) is transmitted for subsequent processing by the main low-pass filter.

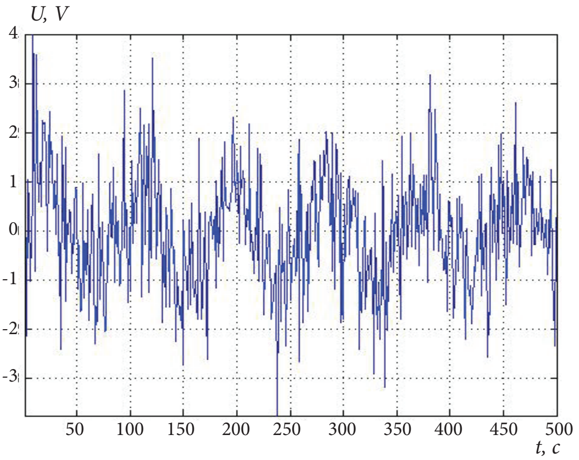

Fig. 4. The signal received at the input of the installation.

During further digital filtering, we considered two possible ways of signal processing: 1) the use of various filters with finite or infinite impulse response; 2) the use of filters based on forward and reverse Fourier transforms. Both of these methods have both disadvantages and advantages. After the experiments, we settled on the second variant of signal processing using the Fourier transform.

Figure 4 shows the test signal from the receiving electrode antennas before the appropriate processing. Figure 5 shows the same signal after hardware and mathematical processing according to the algorithm described above.

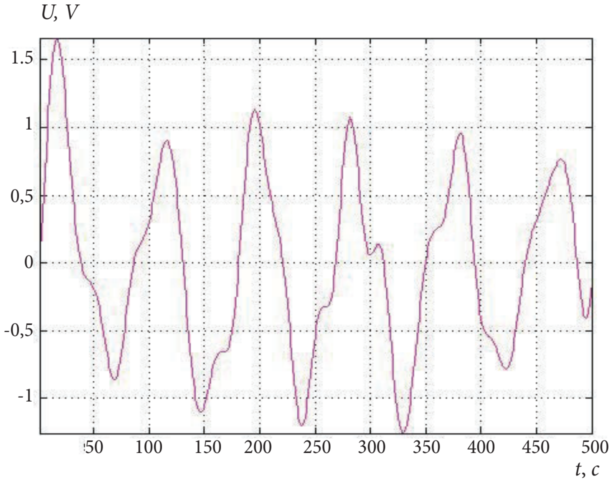

Fig. 5. The signal after appropriate hardware and software filtering.

The given illustrative example clearly demonstrates the achieved effective signal isolation at the noise level using the developed experimental equipment and software.

4 Conclusion

Based on a rigorous solution to the problem of diffraction of the electromagnetic field of a grounded cable on elongated conductive and non-conductive spheroids in an aqueous medium, an experimental implementation of the detection of conductive and non-conductive objects was carried out. For this purpose, a scheme for parallel placement of a generator and two receiving electrode antennas was used and the selection of the passing characteristics of the object against the background of noise by digital hardware and software filtering of the modulated sinusoidal signal. A specialized algorithm for filtering pulse and fluctuation interference was used in the work.

Thus, the proposed practical implementation of the module of the water area protection system makes it possible to reliably detect both a swimmer in a light diving suit and a mobile conductive object in a reservoir with fresh or seawater in shallow water conditions.

References

1. Y. Kuzmin, S. Proshkin, Appl. Sci. **13(3)**, 2012 (2023).
2. E. Ificher, B. Jervis, *Digital signal processing. A practical approach* (Russia, Moscow, Williams Publishing House, 2004).
3. W. Bolton, *Pocket Handbook of a metrological engineer* (Russia, Moscow, Publishing house “Dodeka-XXI”, 2002).

4. S. Safronov, Journal of scientific publications of postgraduates and doctoral students **3**, 206-210 (2008).
5. A.I. Solonina, D.A. Ulakhovich, S.N. Arbuzov, E.B. Solovyova, *Fundamentals of digital signal processing* (Russia, Saint-Petersburg, BHV-Petersburg, 2005).
6. D.G. Letenko, A.S. Ivanov, V.V. Fitsak, Tsvetnye Metally **8**, 46-50 (2023).
7. O.V. Zhdaneev, A.V. Zaitsev, V.M. Lobankov, Journal of Mining Institute **246**, 667-677 (2020).
8. G.S. Grigorev, M.V. Salishchev, N.P. Senchina, Journal of Mining Institute **250**, 492-500 (2021).